International Journal of Microwave and Wireless Technologies

cambridge.org/mrf

A CPW-fed dual band four-port MIMO antenna based on liquid crystal polymer for flexible IoT applications

Jie Zhang, Chengzhu Du, Lingru Pei and Hongye Liu

School of Electronics and Information Engineering, Shanghai University of Electric Power, Shanghai 200090, People's Republic of China

Research Paper

Cite this article: Zhang J, Du C, Pei L, Liu H (2023). A CPW-fed dual band four-port MIMO antenna based on liquid crystal polymer for flexible IoT applications. *International Journal of Microwave and Wireless Technologies* **15**, 1570–1578. https://doi.org/10.1017/S1759078723000223

Received: 26 September 2022
Revised: 28 February 2023
Accepted: 8 March 2023

Key words:
CPW; dual band; flexible antenna; IoT; liquid crystal polymer; MIMO

Author for correspondence:
Chengzhu Du, E-mail: duchengzhu@163.com

Abstract

A 2 × 2 dual band MIMO flexible antenna with a low profile and CPW feeding is designed for Internet of Things (IoT) domains, operating in 5G (3.3–3.6/4.8–5.0 GHz), WiMAX (5.25–5.85 GHz) and WLAN (5.15–5.35/5.725–5.825 GHz) bands. Two resonant frequencies are generated by *L*-shaped branches and a rectangular monopole. The mentioned MIMO antenna comprises four elements arranged vertically. With the addition of an orthogonal branch, significant isolation is attained, which exceeds 21 dB in the entire bands. The four-element MIMO antenna is fabricated and experimented to analyze the performance. According to the measurement, the antenna can operate bandwidth covering 3.156–3.84 GHz (19.55%) and 4.638–6.348 GHz (31.13%). Furthermore, the provided four-element MIMO antenna possesses a number of advantageous properties, such as ECC, DG, and TARC, indicating its suitability for 5G/WiMAX/WLAN applications. In accordance with the results of bending measurement and human body influence, it is evident that the presented liquid crystal polymer antenna could be an ideal candidate for integrating into wearable 5G/WiMAX/WLAN devices.

Introduction

The Internet of Things (IoT) has become a hot research area nowadays [1–3], due to the rapid growth of modern communication technologies. As more smart devices require Internet access, the IoT is gaining popularity to meet the needs of people's convenience life. The IoT system is vital for many applications such as intelligent home, intelligent healthcare, intelligent cities and intelligent grid. Based on 5G technology, massive devices in small sizes will be connected to the Internet by IoT systems. MIMO antenna systems can optimize the utilization of space resources by enhancing spectrum efficiency and minimizing co-channel interference [4], which makes them ideal for IoT applications.

Due to their small size, light weight, and bending capacity, flexible antennas have been widely used in wireless body area network IoT applications and other domains [5–8]. There have been a number of proposals for MIMO antennas utilizing flexible materials [9–17]. In [9], a UWB MIMO antenna is demonstrated integrating with DGS based on the jeans working in UWB and WLAN with excellent isolation of 32 dB. In [10], a MIMO antenna based on felt with an overall size of 38.1 × 38.1 × 2 mm^3 covering 2.4–2.65 GHz. A MIMO antenna fed by coaxial has been designed using jeans as substrate [11]. The above MIMO antenna configurations with two ports are not suitable for handling additional users. Antennas in [12–17] have great performance with four elements. A flexible substrate has been used in [12, 13] for designing the antenna, which is capable of operating when folded. The antenna in [14] can work in 2.21–6 GHz, which is based on a flexible AgHT-4 substrate. In [15, 16], four-element MIMO antennas using jeans with great isolation have been proposed by Sourav Roy and his team. In [17], a four-port MIMO antenna has been printed on a flexible substrate for 5G NR, Wi-Fi 6, sub-1 GHz and sub-6 GHz applications, but has poor isolation of 10 dB.

The paper proposes a flexible CPW-fed four-element antenna that is fabricated by using an liquid crystal polymer (LCP) substrate and tested in a microwave anechoic chamber. LCP has the properties of thermal stability, bendability, low moisture absorbency and stable dielectric constant, which makes the presented antenna an ideal candidate for IoT applications. The oversize is 60 × 60 × 0.1 mm^3. To achieve high port isolation, an orthogonal branch is added in the antenna's center, which connects the ground of different elements. The actual measurement indicates that the operating bands of the four-element MIMO antenna are 3.156–3.84/4.638–6.348 GHz with great isolation of −21 dB, meeting the many spectrum requirements such as 5G, WLAN, WiMAX and so on. Additionally, the antenna performs well in bowed conditions and on the body of the user.

Antenna design

Single element antenna

Figure 1 describes the initial geometry of the single antenna element and its *S*-parameter, the *L*-shaped branch of the antenna can resonate at 3.5 GHz, while the rectangular patch of the antenna can resonate at 5.5 GHz. The S_{11} (<−10 dB) range of the antenna is 3.23 to 3.92 GHz and 4.43 to 7.17 GHz, which can meet the required frequency range of 3.5 and 5.5 GHz.

Four-element MIMO antenna

An illustration of the geometry of the provided MIMO antenna is exhibited in Fig. 2. It is fed by a coplanar waveguide and printed on a 0.1 mm thick LCP substrate which has a relative dielectric constant = 2.9 and loss tangent = 0.002. It comprises four vertically placed radiation elements and an orthogonal branch is located at the center of the four units to reduce unnecessary coupling, which connects the ground between them. The two resonate points are realized by radiation units comprising a rectangular monopole and an *L*-shaped branch. All elements are fed by CPW. The following are the final values of simulation and optimization of the different geometric parameters using HFSS: $W = 60$ mm, $W_1 = 10$ mm, $W_2 = 5$ mm, $W_d = 8.3$ mm, $L = 60$ mm, $L_1 = 14$ mm, $L_2 = 13$ mm, $L_3 = 50$ mm.

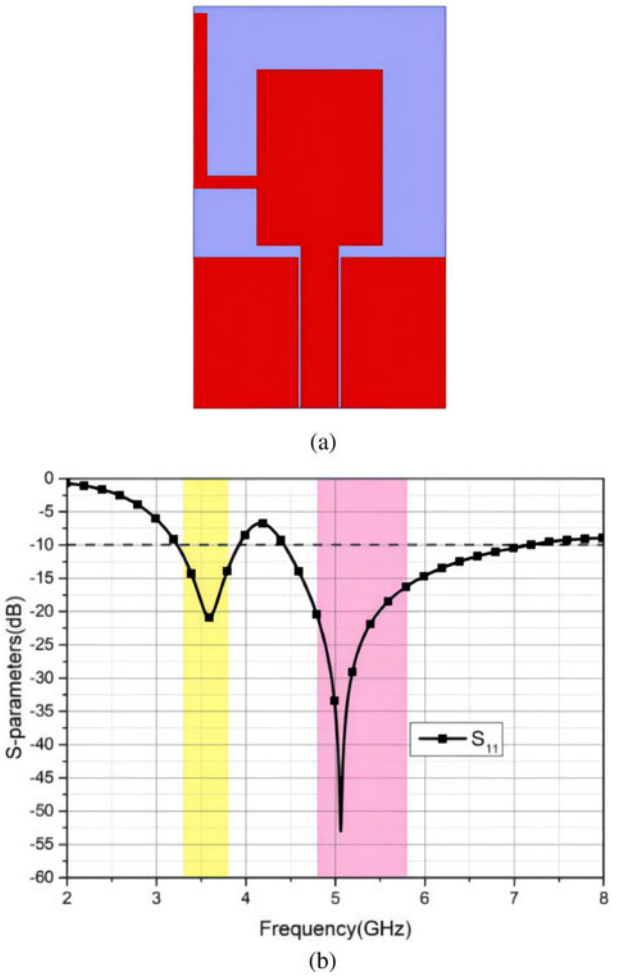

Fig. 1. The structure and *S*-parameter of single antenna. (a) Single antenna structure (b) S_{11} of the single antenna.

Isolation structure analysis

A diagram of the decoupling structure design process is exhibited in Fig. 3. Ant-1 is comprised of four elements vertically arranged to each other without isolation branches. Ant-2 adds an orthogonal branch placed in the center which connects the ground of different elements based on Ant-1.

Figure 4 depicts the simulated scattering parameters of both Ant-1 and Ant-2. Because the placement of four elements is centrosymmetric, the verdict of $S_{11} = S_{22} = S_{33} = S_{44}$, $S_{12} = S_{14} = S_{23} = S_{34} = S_{43} = S_{32} = S_{41} = S_{21}$ and $S_{13} = S_{24} = S_{42} = S_{31}$ can be obtained. Due to orthogonality, the perpendicular arrangement of the antenna elements has degraded the coupling between adjacent elements. However, S_{31} is higher than −15 dB in the low-frequency part. The addition of the isolation branch significantly has decreased the values of S_{31}, which means the coupling of two diagonally placed elements has reduced. Even though isolation branches cause coupling between orthogonal antenna elements, S_{21} still meets working requirements. By adding the isolation branch, the operating band ($S_{11} < -10$ dB) covers 3.05–3.71 and 3.89–6.72 GHz, while the values of S_{21} and S_{31} are all less than −21 dB. At the same time, the branch connects the ground of different antenna units so that each port can obtain the same voltage. According to Fig. 5, the distinction of current distribution between Ant-1 and Ant-2 at different frequencies indicates that the mutual coupling current decreases significantly after adding the isolation branch.

Experimental verification

S-parameter

The introduced four-element flexible antenna was manufactured and tested. In Fig. 6, both simulated and tested *S*-parameter curves are compared. The antenna operated in 3.156–3.84 GHz (19.55%) and 4.638–6.348 GHz (31.13%), covering 5G, WLAN and WiMAX. Figure 6(b) manifests the isolation measured on the operating frequency band is less than −21 dB. Compared to the simulated results, the actual measurement follows a similar trend. In addition, slight variations in curves can be attributed to fabrication errors, the loss of antenna test connector, and a change in the shape of the substrate.

Radiation patterns

As depicted in Fig. 7, the radiation patterns were simulated and measured at 3.5 and 5.5 GHz, in E-plane and H-plane respectively. Taking into account the symmetrical design, only the case where Port 1 is used as the excitation source and the other Ports as load has been tested. The simulated and measured co-polarization patterns are normalized. The 2-D patterns exhibit that both resonance points emit bidirectional radiation in E-plane while emitting omnidirectional radiation in H-plane. At these frequencies, the cross-polarization is generally lower than the co-polarization except for a few degrees. The measurement results are distorted because there is large interference in the 2-D Microwave Anechoic Chamber. At the same time, no power amplifier is used for the antenna, which also leads to a certain deviation between the simulated pattern and the measured one.

https://doi.org/10.1017/S1759078723000223 Published online by Cambridge University Press

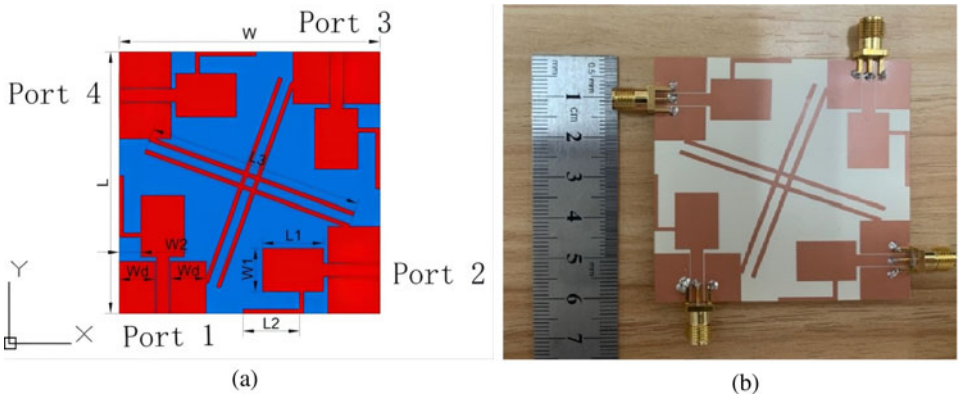

Fig. 2. The introduced MIMO antenna. (a) Geometrical details (b) Fabricated antenna.

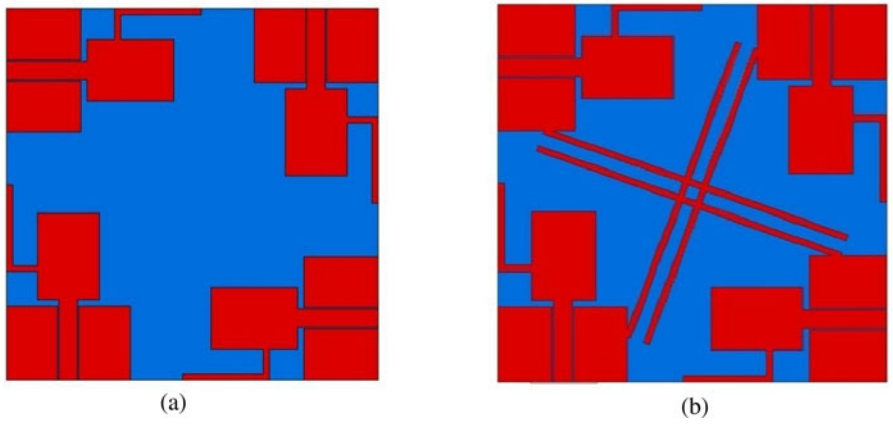

Fig. 3. Design process. (a) Ant-1 (b) Ant-2.

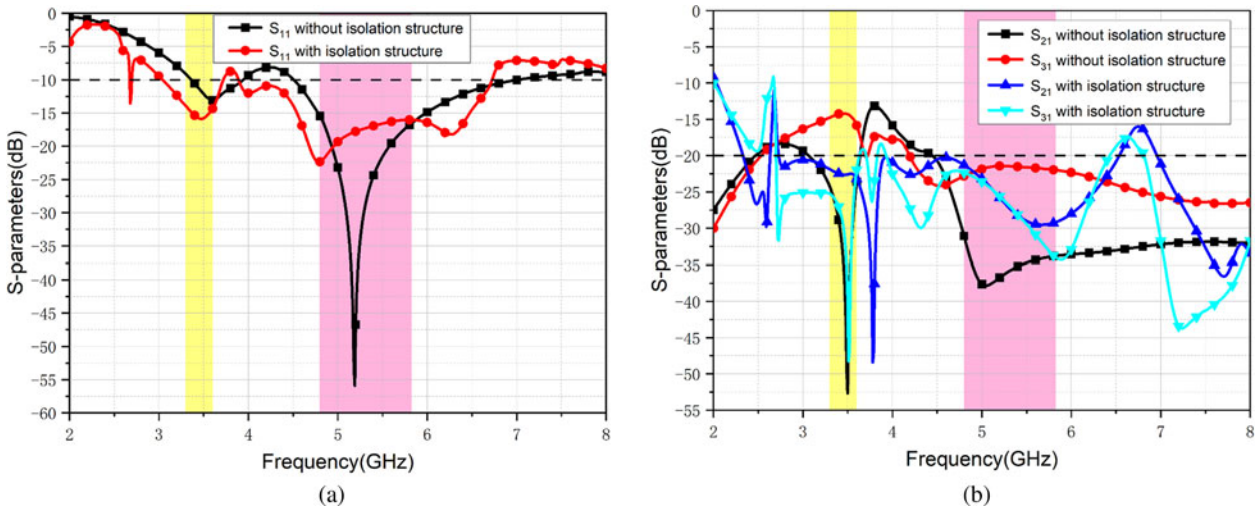

Fig. 4. Simulated *S*-parameters. (a) S_{11} (b) S_{21} and S_{31}.

ECC and DG of antenna

As a basic parameter, envelope correlation coefficient (ECC) is used in MIMO system to estimate the correlation degree between different antenna elements, which can be calculated as follows [18]:

$$\rho_e(i,j,N) = \left| \frac{\sum_{n=1}^{N} S_{i,n}^{*} S_{n,j}}{\left| \prod_{k=i,j} \left(1 - \sum_{n=1}^{N} S_{k,n}^{*} S_{n,k}\right) \right|^{1/2}} \right|^2 \quad (1)$$

The antenna must have a relatively high efficiency to maintain the validity of equation (1). By using the following equation (2), then, we can also calculate the ECC more accurately based on the far-field radiation:

$$\rho_e(i,j) = \frac{\left| \iint_{4\pi} \vec{F}_i(\theta,\phi) \cdot \vec{F}_j(\theta,\phi) d\Omega \right|^2}{\iint_{4\pi} \left| \vec{F}_i(\theta,\phi) \right|^2 d\Omega \cdot \iint_{4\pi} \left| \vec{F}_j(\theta,\phi) \right|^2 d\Omega} \quad (2)$$

https://doi.org/10.1017/S1759078723000223 Published online by Cambridge University Press

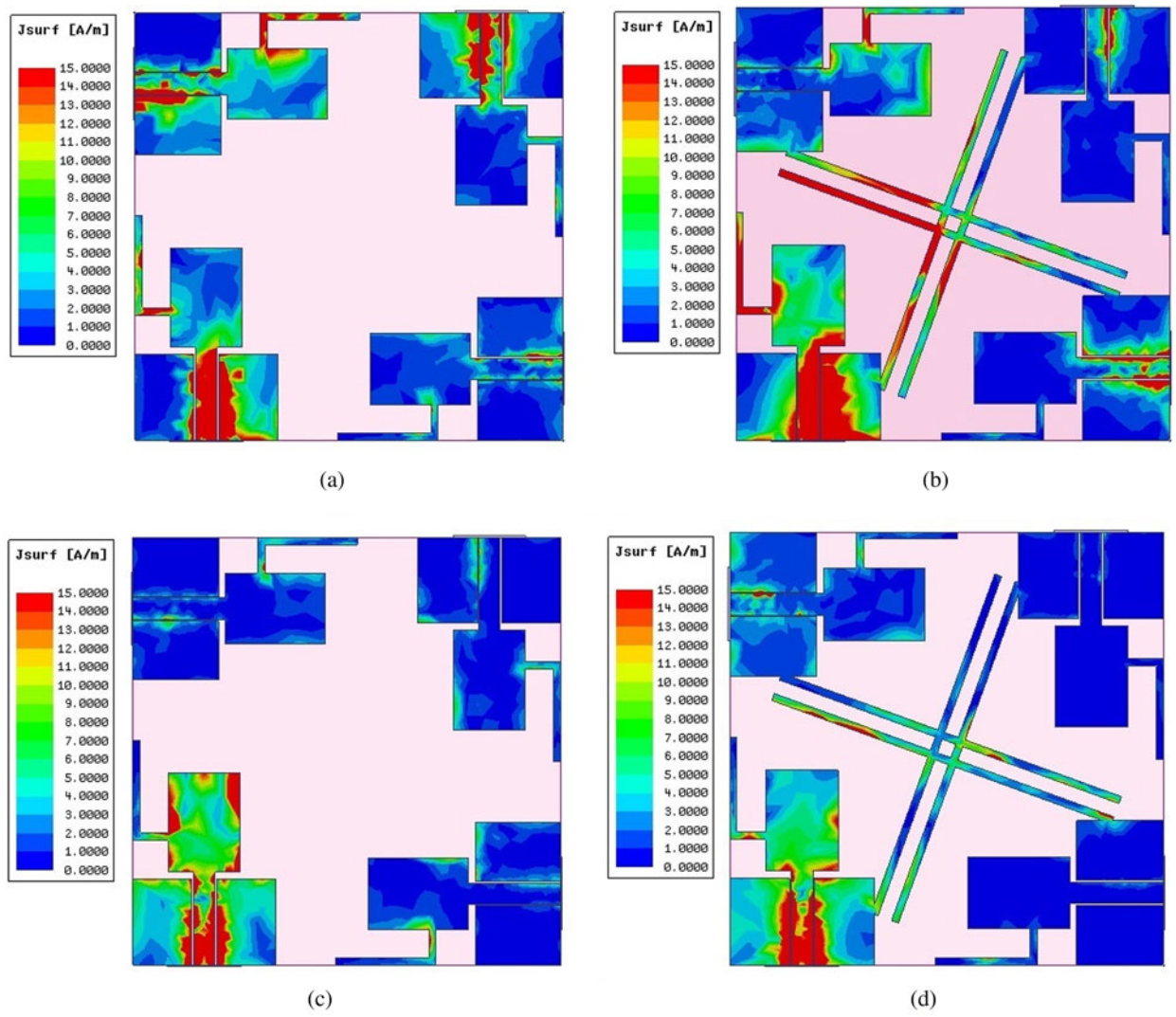

Fig. 5. Current distributions. (a) Ant-1 at 3.5 GHz (b) Ant-2 at 3.5 GHz (c) Ant-1 at 5.5 GHz (d) Ant-2 at 5.5 GHz.

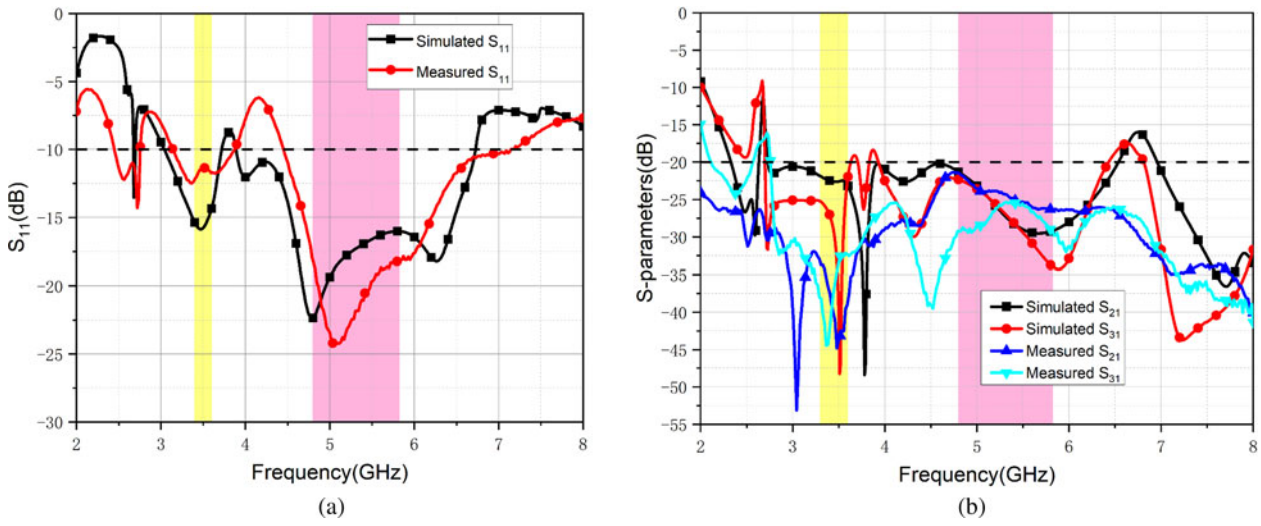

Fig. 6. Simulated and measured *S*-parameters. (a) S_{11} (b) S_{21} and S_{31}.

https://doi.org/10.1017/S1759078723000223 Published online by Cambridge University Press

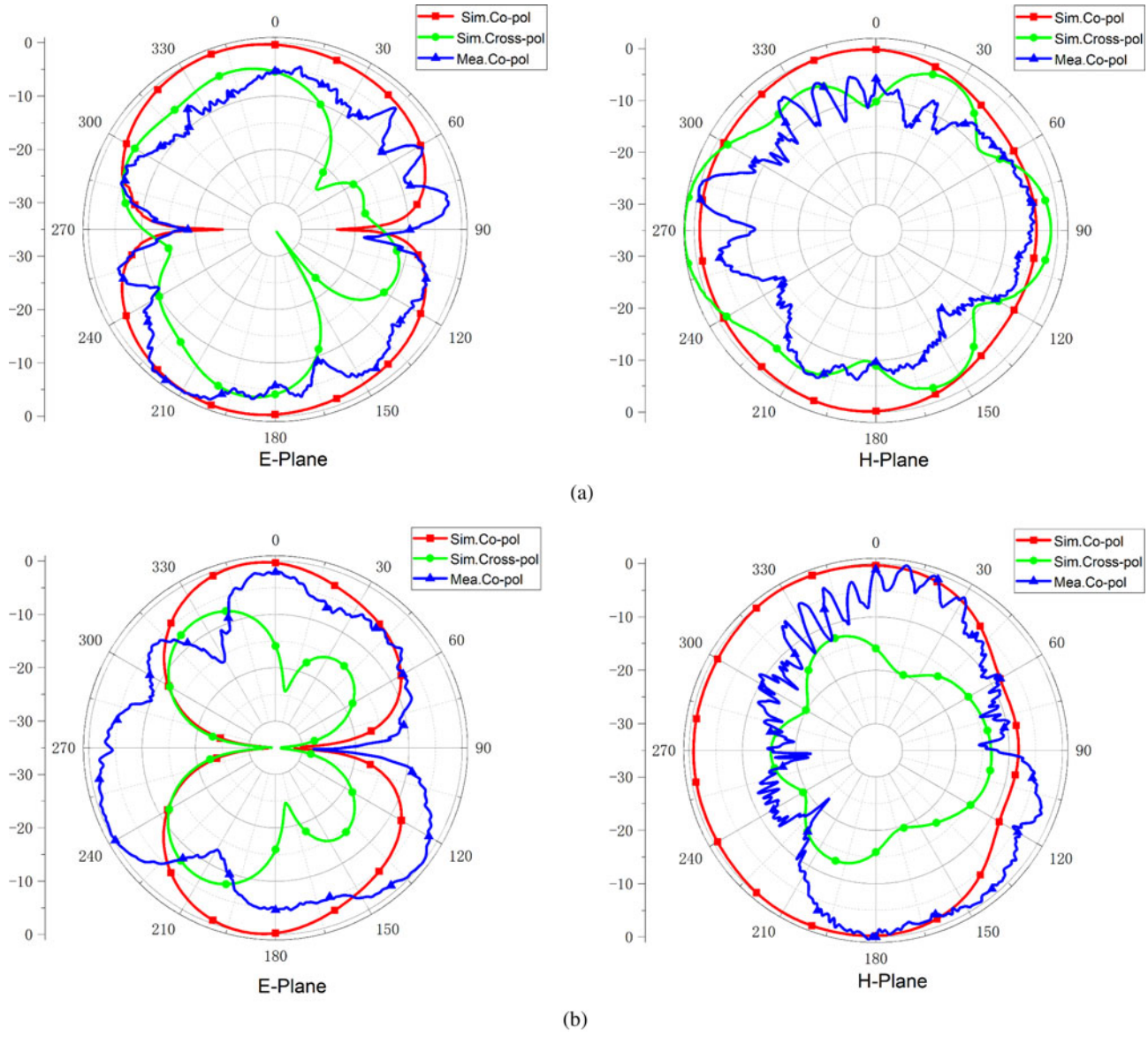

Fig. 7. Radiation patterns. (a) 3.5 GHz (b) 5.5 GHz.

At the same time, diversity gain (DG) is also crucial when evaluating MIMO antenna characteristics. The DG can be calculated as [19]:

$$DG = 10\sqrt{1 - ECC^2} \tag{3}$$

Generally, in the working band, the ECC value should not exceed 0.5, while the DG is larger than 9.5, which can be used in practice. Figure 8 demonstrates that the presented antenna possesses a good ECC less than 0.12, exceeding the requirement by a wide margin.

In Fig. 9, DG curves during 2–8 GHz show a high value of DG, better than 9.93.

Gain

Figure 10 shows the peak gain of simulation and measurement covering 3.0–6.0 GHz. In these results, the measured peak gain is about 4 dB for 3.5 GHz and 4.8 dB for 5.5 GHz. Besides, the gain of measurement displays a lower level compared with that of simulation, due to the uncertainty of the environment and the difference of measurement.

TARC (total active reflection coefficient)

TARC is another vital indicator, predicting the performance of MIMO system, which can be expressed as [20]:

$$TARC = N^{-1/2}\sqrt{\sum_{i=1}^{N}\left|\sum_{k=1}^{N} S_{ik}e^{j\theta_{k-1}}\right|^2} \tag{4}$$

In this expression, θ stands for the excited phase angle. Seven phase angles from 0° to 180° are picked to analyze the properties of the proposed four-element antenna. Figure 11 depicts the values of measured TARC between 2.0 to 8.0 GHz. The measured TARC is less than −10 dB over the functioning bands, indicating that the MIMO antenna has stable characteristics and allowable performance.

https://doi.org/10.1017/S1759078723000223 Published online by Cambridge University Press

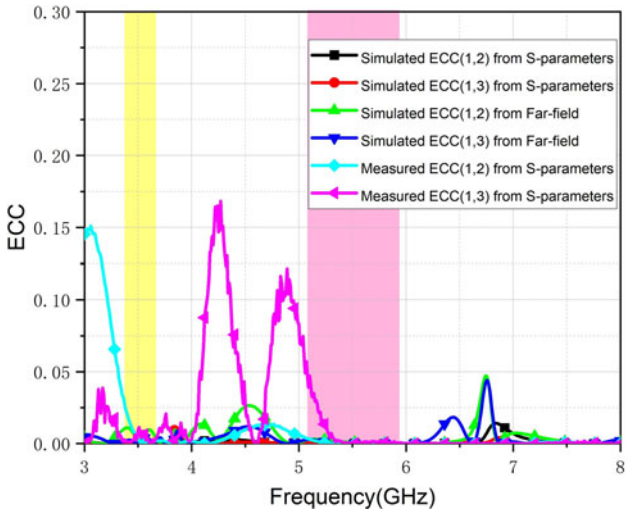

Fig. 8. ECC the of introduced antenna.

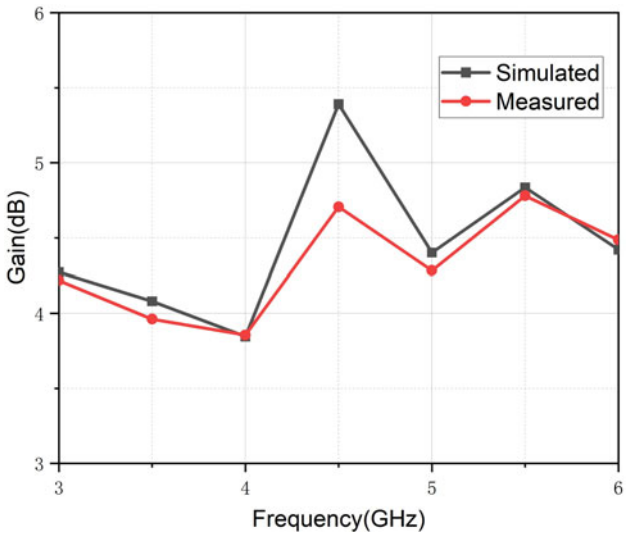

Fig. 10. Simulated and measured gain.

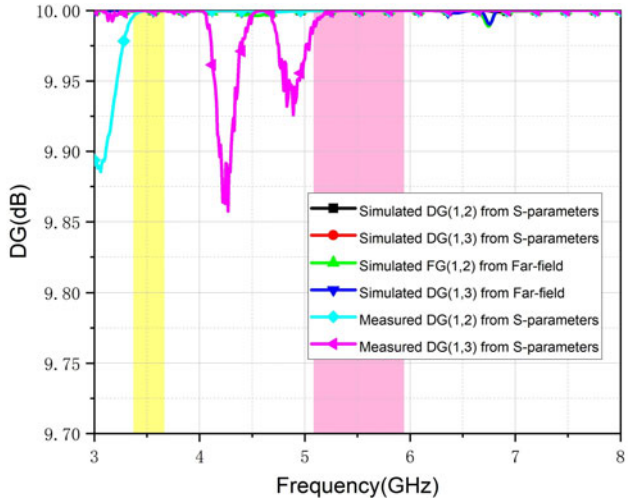

Fig. 9. DG of the introduced antenna.

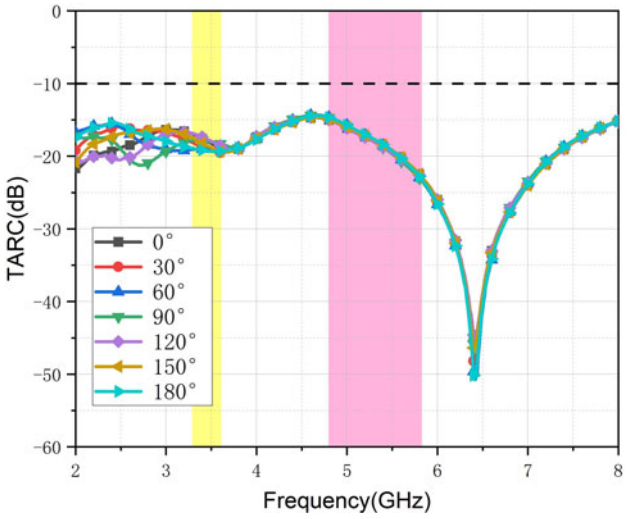

Fig. 11. Measured curves of TARC in different degrees.

Flexibility analysis

The performance of a flexible MIMO antenna under bending conditions is an important metric. The *S*-parameters of this presented four-port flexible antenna are tested when the antenna is fixed on various cylinders with two curvatures ($R = 30$ mm and $R = 45$ mm) along E-plane or H-plane, respectively. Figure 12 depicts the results of return loss and isolation in different conditions. After bending, the antenna retains its original bandwidth. In the low-frequency band, the isolation of measurement is less than −23 dB, while that does not exceed −15 dB in the high-frequency part, which meets the practical standards. The curves of S_{21}, S_{31} and S_{41} show the proposed four-element antenna exhibits good isolation at bowed conditions.

Effects of human body

Since the proposed antenna is a potential candidate for IoT and wearable fields, it is necessary to study the interaction between it and human tissue. The Specific Absorption Rate (SAR) is a vital parameter towards quantifying the effects of antenna radiation on humans. A human tissue model made up of four layers is designed by HFSS. Figure 13 depicts the model and Table 1 contains its associated parameters.

Parameter *H* represents the distance from the tissue model to an antenna. It is described in Table 2 that maximum SAR values of the presented antenna were attained in various conditions. The simulated values all meet the European Union Standard (2 W/kg/10 g).

When the antenna is worn on the arm, chest and thigh, the tested results of scattering parameters are depicted in the following Fig. 14, which indicates that the presented four-element antenna is still in compliance with the working requirements.

Performance comparison

In Table 3, a comparison is shown between the proposed flexible dual band four-element MIMO antenna and previous designs.

https://doi.org/10.1017/S1759078723000223 Published online by Cambridge University Press

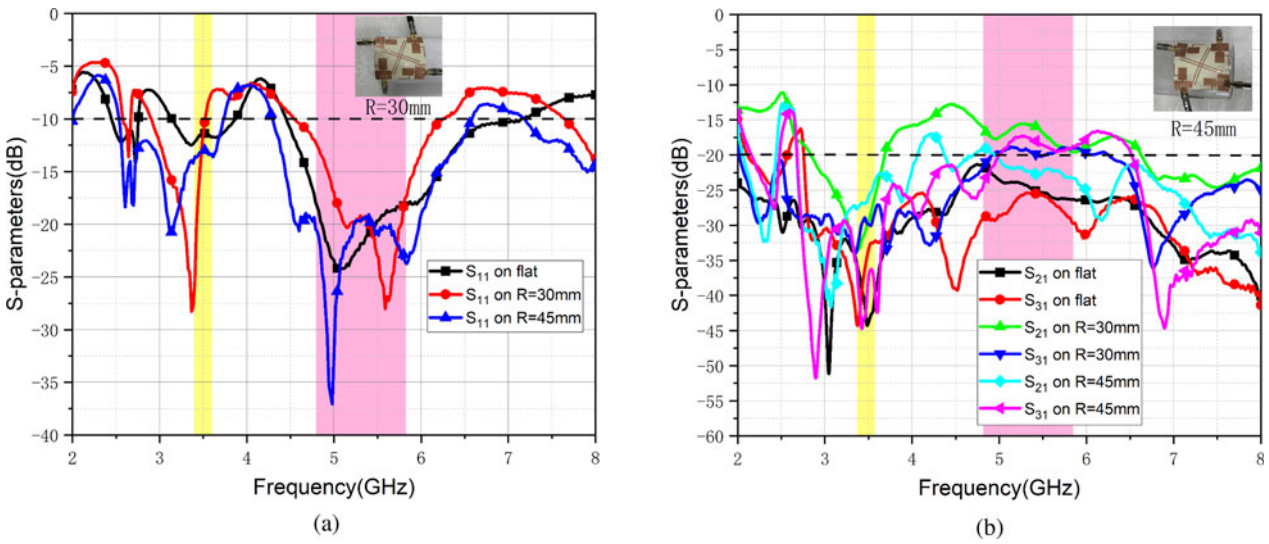

Fig. 12. *S*-parameters in different bending conditions. (a) S_{11} (b) S_{21} and S_{31}.

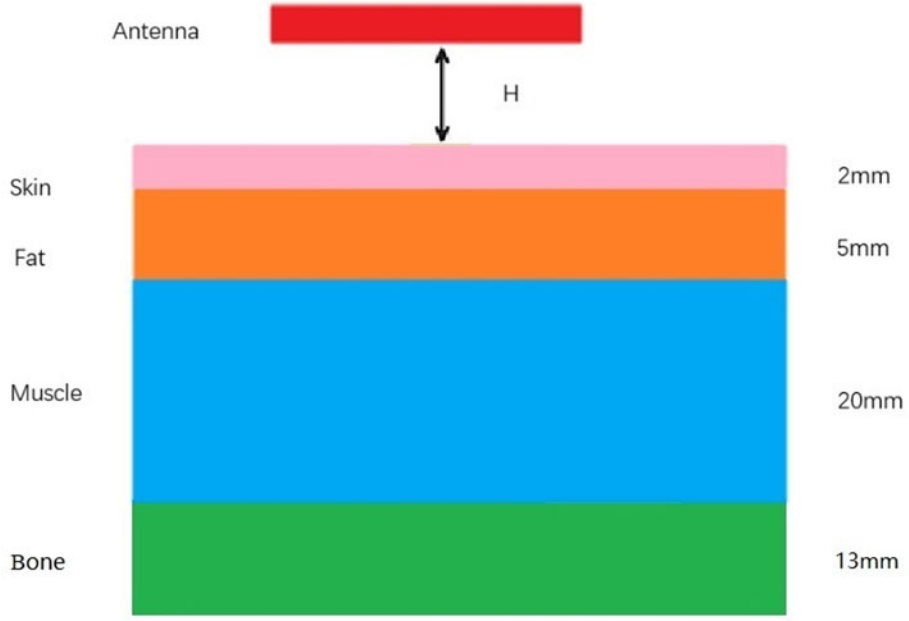

Fig. 13. The human body approaching the antenna model.

Table 1. Characteristics of different tissues of the human body

	Bone	Muscle	Fat	Skin
ϵ_r	18.49	52.67	5.27	37.95
σ (S/m)	0.82	1.77	0.11	1.49
Density (kg/m^3)	1008	1006	900	1001
Thickness (mm)	13	20	5	2

Table 2. Maximum SAR values on various conditions

Frequency (GHz)	H(mm)	SAR (W/Kg/10 g)
3.5	1	0.49
	3	0.13
	5	0.17
5.5	1	1.21
	3	0.69
	5	0.52

The antennas of the literature [10, 11] are only two-port antennas. Thus, their transmission capacity is lower than the one presented. Antennas in [12, 16, 17] are larger than the proposed one. The antenna presented here has better isolation than those in [14, 15]. The table reveals that the introduced flexible MIMO antenna shows a splendid capability with low values of ECC, high isolation and good SAR, which makes it an ideal candidate for IoT devices.

https://doi.org/10.1017/S1759078723000223 Published online by Cambridge University Press

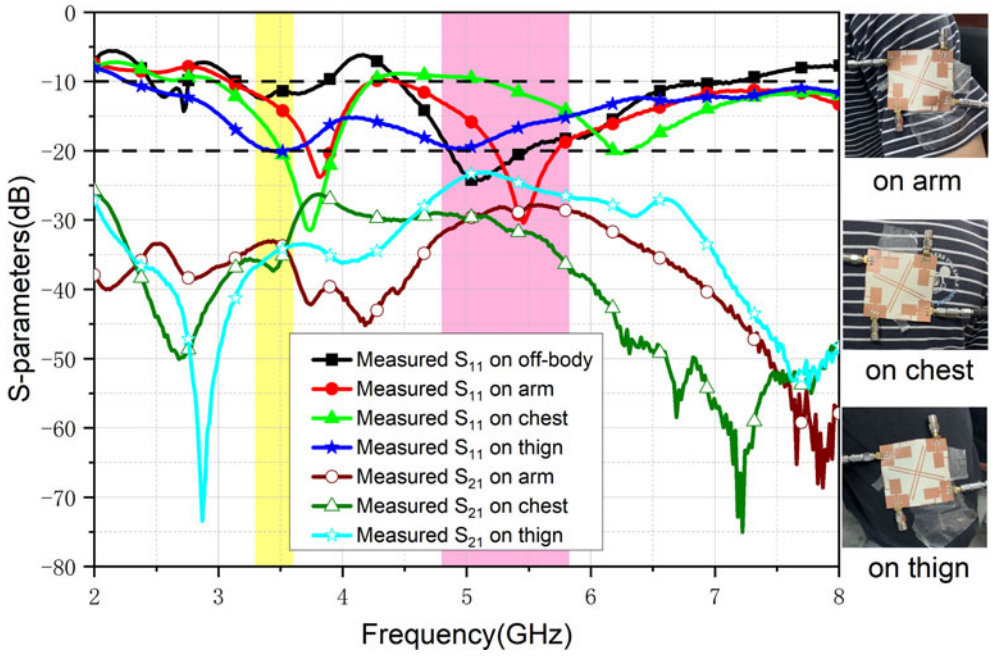

Fig. 14. The tested performance on human body.

Table 3. Comparison between the designed antenna and others

Ref.	No. of ports	Size (mm^3)	Feeding method	Substrate	Bands (GHz)	Iso. (dB)	ECC	DG
[10]	2	38.1 × 38.1 × 2	CPW	Felt	2.4–2.65	10	<0.01	–
[11]	2	101.9 × 92.3 × 3	Coaxial	Felt	2.4–2.5	20	–	–
					5.2–5.8			
[12]	4	168 × 96 × 1.2	Microstrip	Felt	1.4–5	15	<0.8	–
[14]	4	66 × 45 × 0.625	Microstrip	AgHT-4	2.21–6	15	<0.016	9.9
[15]	4	55 × 58 × 1.4	Microstrip	Jeans	2.74–4.41	19	<0.2	>9.6
[16]	4	110 × 97 × 1.4	Microstrip	Jeans	1.5–3.8	24	<0.1	9.9
					4.1–6.1			
[17]	4	180 × 180 × 1.52	CPW	Rogers RO3003	0.7–1.01	10	<0.5	–
					2.6–3.18			
					5.3–6.06			
					6.7–6.94			
Prop.	4	60 × 60 × 0.1	CPW	LCP	3.156–3.84	21	<0.12	>9.9
					4.638–6.348			

Conclusion

A compact CPW-fed flexible dual band four-element MIMO antenna is presented in this work. The operating band is 3.156–3.84 (19.55%)/4.638–6.348 (31.13%), which is compatible with wireless spectrum such as 5G, WLAN, WiMAX, etc. The addition of an orthogonal branch accomplishes decoupling. Therefore, the tested isolation exceeds 31 dB within 3.5 GHz and 21 dB within 5.5 GHz, respectively. Moreover, the flexible four-port antenna exhibits that ECC is less than 0.12, the DG exceeds 9.93, and the TARC curves display excellent characteristics, which indicates it is capable of supporting 5G/WiMAX/WLAN communications. Owing to the bending resistance and stability, the introduced antenna is expected to function in the wearable technology and IoT domains.

Data. Data sharing not applicable to this article as no datasets were generated or analyzed during the current study.

Acknowledgements. The authors would like to thank the CETC Shanghai Microwave Communication Co., Ltd. for providing measure facility.

Author contributions. Hongye Liu and Chengzhu Du derived the theory, Jie Zhang and Lingru Pei performed the simulations. All authors contributed equally to analyzing data and reaching conclusions, and in writing the paper.

https://doi.org/10.1017/S1759078723000223 Published online by Cambridge University Press

Financial support. This research received no specific grant from any funding agency, commercial or not-for-profit sectors.

Conflict of interest. The authors report no conflict of interest.

References

1. **Olan-Nunez KN, Murphy-Arteaga RS and Colmn-Beltran E** (2020) Miniature patch and slot microstrip arrays for IoT and ISM band applications. *IEEE Access* **8**, 102846–102854.
2. **Nagendra R and Swarnalatha S** (2022) Design and performance of four port MIMO antenna for IOT applications. *ICT Express* **8**, 235–238.
3. **Kulkarni P and Srinivasan R** (2021) Compact polarization diversity patch antenna in L and WiMAX bands for IoT applications. *AEU – International Journal of Electronics and Communications* **136**, 153722.
4. **Bengtsson EL, Rusek F, Malkowsky S, Tufvesson F, Karlsson PC and Edfors O** (2017) A simulation framework for multiple-antenna terminals in 5G massive MIMO systems. *IEEE Access* **5**, 26819–26831.
5. **Du C and Jin G** (2021) A compact CPW-fed band-notched UWB-MIMO flexible antenna for WBAN application. *Journal of Electromagnetic Waves and Applications* **35**, 1046–1058.
6. **Kim RH, Tao H, Kim TI, Zhang Y, Kim S, Panilaitis B, Yang M, Kim DH, Jung BH and Rogers JA** (2012) Materials and designs for wirelessly powered implantable light-emitting systems. *Small* **8**, 2812–2818.
7. **Borna A and Najafi K** (2013) A low power light weight wireless multichannel microsystem for reliable neural recording. *IEEE Journal of Solid-State Circuits* **9**, 439–451.
8. **Kiourti A and Nikita KS** (2012) A review of implantable patch antennas for biomedical telemetry: challenges and solutions. *IEEE Antennas Propagation Magazine* **54**, 210–228.
9. **Biswas AK and Chakraborty U** (2019) Investigation on decoupling of wide band wearable multiple-input multiple-output antenna elements using microstrip neutralization line. *International Journal of RF and Microwave Computer-Aided Engineering* **29**, e21723.
10. **Li H, Sun S, Wang B and Wu F** (2018) Design of compact single-layer textile MIMO antenna for wearable applications. *IEEE Transactions on Antennas and Propagation* **66**, 3136–3141.
11. **Yan S, Soh PJ and Vandenbosch GA** (2015) Dual-band textile MIMO antenna based on substrate-integrated waveguide (SIW) technology. *IEEE Transactions on Antennas and Propagation* **63**, 4640–4647.
12. **Choi S and Lim S** (2015) Foldable thin electro-textile antenna array for 4×4 multiple-input multiple-output mobile router applications. *Journal of Electromagnetic Waves and Applications* **29**, 375–385.
13. **Elwi TA** (2018) A miniaturized folded antenna array for MIMO applications. *Wireless Personal Communications* **98**, 1871–1883.
14. **Desai A, Palandoken M, Kulkarni J, Byun G and Nguyen TK** (2021) Wideband flexible/transparent connected-ground MIMO antennas for sub-6 GHz 5G and WLAN applications. *IEEE Access* **9**, 147003–147015.
15. **Roy S, Biswas AK, Ghosh S, Chakraborty U and Sarkhel A** (2021) Isolation improvement of dual-/quad-element textile MIMO antenna for 5G application. *Journal of Electromagnetic Waves and Applications* **35**, 1337–1353.
16. **Roy S, Ghosh S, Pattanayak SS and Chakarborty U** (2020) Dual-polarized textile-based two/four element MIMO antenna with improved isolation for dual wideband application. *International Journal of RF and Microwave Computer-Aided Engineering* **30**, e22292.
17. **Jha KR, Jibran ZP, Singh C and Sharma SK** (2021) 4-port MIMO antenna using common radiator on a flexible substrate for sub-1GHz, sub-6GHz 5G NR, and Wi-Fi 6 applications. *IEEE Open Journal of Antennas and Propagation* **2**, 689–701.
18. **Ikram M, Nguyen-Trong N and Abbosh AM** (2019) Realization of a tapered slot array as both decoupling and radiating structure for 4G/5G wireless devices. *IEEE Access* **7**, 159112–159118.
19. **Tian R, Lau BK and Ying Z** (2011) Multiplexing efficiency of MIMO antennas. *IEEE Antennas and Wireless Propagation Letters* **10**, 183–186.
20. **Dkiouak A, Zakriti A and El Ouahabi M** (2020) Design of a compact dual-band MIMO antenna with high isolation for WLAN and X-band satellite by using orthogonal polarization. *Journal of Electromagnetic Waves and Applications* **34**, 1254–1267.

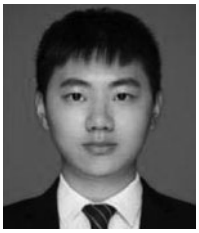

Jie Zhang was born in ZhouNing, FuJian Province, China in 1996. He received the B.S. degree from the Shanghai University of Electric Power in 2020. He is currently pursuing the M.S. degree in College of Electronics and Information Engineering, Shanghai University of Electric Power. His research interests include CPW-UWB-MIMO antenna, flexible antenna and SIW millimeter wave antenna.

Chengzhu Du was born in Haikou, Hainan Province, China. She received the B.S. degree from the Xidian University, M.S. degree from Nanjing University of Posts and Telecommunications and Ph.D. degree from Shanghai University, in 1995, 2003, and 2012, respectively, all in electromagnetic wave and microwave technology. She is currently an associate professor of Shanghai University of Electric Power. Her research interests include flexible antenna and textile antenna, multiband and wideband antennas, and MIMO technologies.

Lingru Pei was born in Jinzhong, Shanxi Province, China in 1998. She received the B.S. degree from the Shanghai University of Electric Power in 2020. She is currently pursuing the M.S. degree in College of Electronics and Information Engineering, Shanghai University of Electric Power. Her research interests include UWB-MIMO antenna, flexible antenna and multiband MIMO antenna.

Hongye Liu was born in Zigong, Sichuan Province, China in 1996. She received the B.S. degree from the Southwest Jiaotong University in 2018. She is currently pursuing the M.S. degree in College of Electronics and Information Engineering, Shanghai University of Electric Power. Her research interests include MIMO antenna, flexible antenna.

https://doi.org/10.1017/S1759078723000223 Published online by Cambridge University Press